Deposition Chemistry of $Cu[OCH(Me)CH_2NMe_2]_2$ over Mesoporous Silica

Guoying Zhang, Xuxu Wang,* Jinlin Long, Lili Xie, Zhengxin Ding, Ling Wu, Zhaohui Li, and Xianzhi Fu*

Research Institute of Photocatalysis, State Key Laboratory Breeding Base of Photocatalysis, Fuzhou University, Fuzhou, 350002, China

Received September 23, 2007. Revised Manuscript Received February 13, 2008

The deposition of an organic copper precursor $Cu[OCHMeCH_2NMe_2]_2$ on the surface of mesoporous silica MCM-41 dehydrated at 773 K was studied under high-vacuum conditions by infrared spectroscopy combined with elemental analysis, X-ray absorption spectroscopy (XAS), thermogravimetric analysis (TG), temperature-programmed decomposition (TPD), and X-ray photoelectron spectroscopy (XPS). It is revealed that the copper precursor is chemically adsorbed on the surface of MCM-41 to form a stable surface copper complex (SC1) coordinated with two framework oxygen atoms by ligand exchange at temperatures below 423 K. The surface copper complex is easily decomposed into Cu(I) and Cu(0) via a successive two-step pathway upon heating at temperatures beyond 423 K. IR and TPD results indicate that the first-step decomposition occurs at the temperature range from 423 to 523 K, where the surface complex SC1 loses one organic ligand and one methane molecule, leading to formation of a surface intermediate complex (SC2) with a Schiff base ligand. The second-step decomposition starts at 523 K, where the complex (SC2) is transformed to Cu(0) by losing the remanent organic ligand and undergoes a surface intermediate complex (SC3) to form Cu(I) oxide species by a consecutive loss of small molecules. The surface hydroxyl groups participate in the adsorption and reaction of the Cu precursor on the support MCM-41, which is a critical factor to controllable preparation of copper-containing MCM-41 catalysts. The mechanisms of thermolysis are suggested to be distinctly different from its MOCVD pathways reported in the literature.

Introduction

Copper-supported catalysts have been widely used for numerous industrial processes in the past decade due to the high activity and selectivity, such as selective hydrogenation of alkynes and unsaturated carbonyl compounds,[1,2] methanol synthesis,[3] dehydrogenation of alcohols,[4,5] hydrogenolysis of esters,[6] production of hydrogen in fuel cells,[7,8] catalytic reduction of NO_X,[9–12] liquid-phase selective hydroxylation-substituted phenol,[13,14] and hydrogenation of furfural to furfuryl alcohol.[15] Various techniques, such as the sol−gel method,[16,17] microemulsions,[18] and salt impregnation−reduction,[19,20] have been developed for preparation of the copper catalyst systems. Very recently, use of organic copper complexes as precursors for preparation of highly dispersed metal copper or copper oxide catalysts has attracted considerable interest for investigations. Depositing of organic copper precursor on supports is reported to be a facile synthesis technique,[21–26] but only limited information is available on the deposition mechanism. Young et al.[23]

* To whom correspondence should be addressed. E-mail: xwang@fzu.edu.cn, xzfu@fzu.edu.cn.

(1) Ossipoff, N. J.; Cant, N. W. *J. Catal.* **1994**, *148*, 125–133.
(2) Koeppel, R. A.; Wehrli, J. T.; Wainwright, M. S.; Trimma, D. L.; Cant, N. W. *Appl. Catal. A: Gen.* **1994**, *120*, 163–177.
(3) Gotti, A.; Prins, R. *J. Catal.* **1998**, *178*, 511–519.
(4) Fridman, V. Z.; Davydov, A. A.; Titievsky, K. *J. Catal.* **2004**, *222*, 545–557.
(5) Minyukova, T. P.; Simentsova, I. I.; Khasin, A. V.; Shtertser, N. V.; Baronskaya, N. A.; Khassin, A. A.; Yurieva, T. M. *Appl. Catal. A: Gen.* **2002**, *237*, 171–180.
(6) Brands, D. S.; Poels, E. K.; Bliek, A. *Appl. Catal. A: Gen.* **1999**, *184*, 279–289.
(7) Agrell, J.; Birgersson, H.; Boutonnet, M.; Melián-Cabrera, I.; Navarro, R. M.; Fierro, J. L. G. *J. Catal.* **2003**, *219*, 389–403.
(8) Agrell, J.; Hasselbo, K.; Jansson, K.; Järås, S. G.; Boutonnet, M. *Appl. Catal. A: Gen.* **2001**, *211*, 239–250.
(9) Shibata, J.; Shimizu, K.; Satsuma, A.; Hattori, T. *Appl. Catal. B: Environ.* **2002**, *37*, 197–204.
(10) Andersona, J. A.; Alvarezb, C. M.; Mufiozb, M. J. L.; Ramosb, I. R.; Ruiz, A. G. *Appl. Catal. B: Environ.* **1997**, *14*, 189–202.
(11) Capek, L.; Ddeček, J.; Wichterlová, B.; Cider, L.; Jobson, E.; Tokarová, V. *Appl. Catal. B: Environ.* **2005**, *60*, 147–153.
(12) Tomašić, V.; Gomzi, Z.; Zrnčević, S. *Appl. Catal B: Environ.* **1998**, *18*, 233–240.
(13) Fujiyama, H.; Kohara, I.; Iwai, K.; Nishiyama, S.; Tsuruya, S.; Masai, M. *J. Catal.* **1999**, *188*, 417–425.
(14) Franco, L. N.; Perez, I. H.; Pliego, J. A.; Franco, A. M. *Catal. Today* **2002**, *75*, 189–195.
(15) Hao, X. Y.; Zhou, W.; Wang, J. W.; Zhang, Y. Q.; Liu, S. X. *Chem. Lett.* **2005**, *34*, 1000–1001.
(16) Gu, Z.; Hohn, K. L. *Ind. Eng. Chem. Res.* **2004**, *43*, 30–35.
(17) Reyes, P.; Pecchi, G.; Fierro, J. L. G. *Langmuir* **2001**, *17*, 522–527.
(18) Wang, X.; Rodriguez, J. A.; Hanson, J. C.; Gamarra, D.; Arias, A. M.; García, M. F. *J. Phys. Chem. B* **2006**, *110*, 428–434.
(19) Desforges, A.; Deleuze, H.; Monval, O. M.; Backov, R. *Ind. Eng. Chem. Res.* **2005**, *44*, 8521–8529.
(20) Fujiwara, N.; Asaka, K.; Nishimura, Y.; Oguro, K.; Torikai, E. *Chem. Mater.* **2000**, *12*, 1750–1754.
(21) Vertoprakhov, V. N.; Krupoder, S. A. *Russ. Chem. Rev.* **2000**, *69*, 1057–1082.
(22) Goel, S. C.; Kramer, K. S.; Chiang, M. Y.; Buhro, W. E. *Polyhedron* **1990**, *9*, 611–613.
(23) Young, V. L.; Cox, D. F.; Davis, M. E. *Chem. Mater.* **1993**, *5*, 1701–1709.
(24) Becker, R.; Devi, A.; Becker, H. W.; Fischer, R. A. *Chem. Vap. Depos.* **2003**, *9*, 149–156.

10.1021/cm7027228 CCC: $40.75
Published on Web 06/18/2008

suggested that thermal deposition of copper from $Cu(OCH_2CH_2NMe_2)_2$ on the $SrTiO_3$ surface occurred by interdependent β-hydride elimination and reductive elimination reactions. Becker showed that deposition of copper film on SiO_2/Si by MOCVD of $Cu(OCHMeCH_2NMe_2)_2$ follows a similar mechanism.[24] For some congeneric precursors, such as $Cu(OCMe_2CH_2NMe_2)_2$ and $Cu[OC(CF_3)_2CH_2NMe_2]_2$, their decompositions into metal Cu were considered to occur through the dialkylamino group assisted γ-hydrogen elimination reaction and a cooperative $C(\alpha)-C(\beta)$ bond fission reaction followed by the reductive elimination reaction.[27,28] All suggested pathways in the literature are short of detail only by virtue of the results by IR spectroscopic and mass spectroscopic analysis of the accumulate reactor gas phase. On the other hand, these studies do not take into account the effect of support or substrate.

It is well known that the MOCVD process of an organometallic precursor on a solid surface usually takes place in several steps including adsorption and thermal decomposition of the precursor as well as desorption of the products.[29] The surface characteristics of support undoubtedly affect the chemical state and dispersity of the deposits, which are especially important for preparation of catalysts with stable and well-dispersed active phase. The objective of this work is to provide molecular insight into the deposition chemistry of the copper precursor onto a support and the support effect. Adsorption and thermolysis of $Cu(OCHMeCH_2NMe_2)_2$ on the surface of MCM-41 were investigated in detail under vacuum conditions by in situ Fourier transform infrared spectroscopy (FT-IR), atomic absorption spectroscopy (AAS), temperature-programmed decomposition coupled with mass spectroscopy (TPD-MS), X-ray absorption spectroscopy (XAS), and X-ray photoelectron spectroscopy (XPS). MCM-41 was selected as support for three reasons: (i) high specific surface area and wide pore diameter that allow the organometallic molecule to be accessible to its inter surface, (ii) rich and active surface hydroxyl that can strongly interact with the organometallic molecule, and (iii) intrinsic uniformity of porous surface that permits the organometallic molecule to be uniformly dispersed. The results show that $Cu[OCHMeCH_2NMe_2]_2$ undergoes adsorption and stepwise decomposition under participation of the surface hydroxyls of MCM-41 in the temperature range of 298−723 K, which is completely different from its MOCVD pathways reported in the literature.[23] Of the significant intermediates along the proposed thermolysis pathway, two surface complexes (SC1 and SC2) have been observed clearly by IR spectroscopy.

Experimental Section

1. Preparation of MCM-41 and $Cu[OCHMeCH_2NMe_2]_2$. $Na_2Si_3O_7$ and dimethylamino-2-proponol were purchased from Sigma-Aldrich and Merk-Schuchardt, respectively. Other reagents were furnished by Guangzhou Chemical Reagent Corp., China. MCM-41 was prepared by a typical procedure using tetradecyltrimethylammonium bromide as a surfactant and $Na_2Si_3O_7$ as a source of silica followed by calcination under flowing oxygen at 813 K for 20 h.[30] The resulting solid was checked to have good mesoporous structure by powder X-ray diffraction (XRD) and ca. 1000 $m^2\ g^{-1}$ of BET surface area as well as 3.2 nm of BJH porous diameter by N_2 physisorption at 77 K. $Cu[OCHMeCH_2NMe_2]_2$ (Me = CH_3) was synthesized by an alcohol-exchange reaction process described in the literature.[22] Reaction of copper methoxide, $Cu(OMe)_2$, with 1-dimethylamino-2-propanol was performed in pentane at room temperature. After removing the solvent the product was purified by sublimation under vacuum (10^{-4} Torr) at 333 K. The purple solid $Cu[OCHMeCH_2NMe_2]_2$ was obtained, as checked by IR spectrum,[23] and preserved in a glovebox full of N_2 atmosphere to avoid hydrolysis prior to use.

2. Deposition of $Cu[OCHMeCH_2NMe_2]_2$ on MCM-41. Deposition of $Cu[OCHMeCH_2NMe_2]_2$ on MCM-41 was performed in an in situ IR cell connected to a vacuum line. The as-synthesized MCM-41 sample (10−15 mg) was pressed into a thin disk (diameter 18 mm) and loaded in the IR cell equipped with ZnSe or CaF_2 windows and a sample holder. MCM-41 was pretreated in situ under flowing oxygen at 813 K for 20 h and then dehydrated under vacuum (10^{-4} Torr) at 773 K for 4 h. When cooling to room temperature an excess of $Cu[OCHMeCH_2NMe_2]_2$ pentane solution was introduced into the cell with a syringe via a septum. After removing the solvent at room temperature by evacuation, the system was heated to the necessary temperature for the reaction.

3. FT-IR Analysis. The IR spectra of both the solid disk and the gas-phase products were recorded with a Nicollet Nexus 670 FTIR spectrometer.

4. Elemental Analysis. The copper, carbon, and nitrogen contents of the solid product were determined by a PerkinElmer Analyst 800 atomic absorption spectrometer and a Vario EL III elemental analyzer (EA).

5. X-ray Absorption Spectroscopy (XAS). X-ray absorption spectra (Cu K-edge at 8.980 keV) were measured at a beam line U7c station of Hefei Synchrotron Radiation Laboratory (NSRL, China) with a stored electron energy of 0.8 GeV and ring currents between 80 and 250 mA. In all cases, the radiation was monochromatized using a Si(111) double-crystal monochromator. Data on the surface complex and pure copper precursor were all collected in a fluorescence mode at room temperature. The energies of the samples were calibrated using an internal Cu foil standard, assigning the first inflection point to 8979 eV. The energy resolution was 0.3 eV.

Data treatment was carried out using the software package WinXAS 2.0. A linear polynomial was fitted to the pre-edge region and a third-order polynomial to the postedge region for background subtraction and XANES normalization, respectively. The radical structural function (RSF) $FT[\kappa^3\chi(\kappa)]$ was obtained by Fourier transformation of the K^3-weighted experimental function $\chi(\kappa) = (\mu(\kappa) - \mu_0(\kappa))/\mu_0(\kappa)$ multiplied by a Gauss window in the range 2.5−13.8 $Å^{-1}$. The Fourier-filtered data were fitting in R space in the range 1−2 Å. Phase shifts and backscattering amplitudes extracted from the reference material CuO (Cu−O) and the copper precursor (Cu−O and Cu−N) were used to fit the EXAFS data to

(25) Becker, R.; Parala, H.; Hipler, F.; Birkner, A.; Wöll, C.; Hinrichsen, O.; Tkachenko, O. P.; Fischer, R. A. *Angew. Chem., Int. Ed.* **2004**, *43*, 2839–2842.
(26) Lu, L.; Wohlfart, A.; Parala, H.; Birkner, A.; Fischer, R. A. *Chem. Commun.* **2003**, 40–41.
(27) Park, J. W.; Jang, H. S.; Kim, M.; Sung, K.; Lee, S. S.; Chung, T. M.; Koo, S.; Kim, C. G.; Kim, Y. *Inorg. Chem. Commun.* **2004**, *7*, 463–466.
(28) Chi, Y.; Hsu, P. F.; Liu, C. S.; Ching, W. L.; Chou, T. Y.; Carty, A. J.; Peng, S. M.; Lee, G. H.; Chuang, S. H. *J. Mater. Chem.* **2002**, *12*, 3541–3550.
(29) Lai, Y. H.; Yeh, C. T.; Lin, H. J.; Chen, C. T.; Hung, W. H. *J. Phys. Chem. B* **2002**, *106*, 1722–1727.
(30) Wang, X. X.; Lefebvre, F.; Patarin, J.; Basset, J. M. *Microporous Mesoporous Mater.* **2001**, *42*, 269–276.

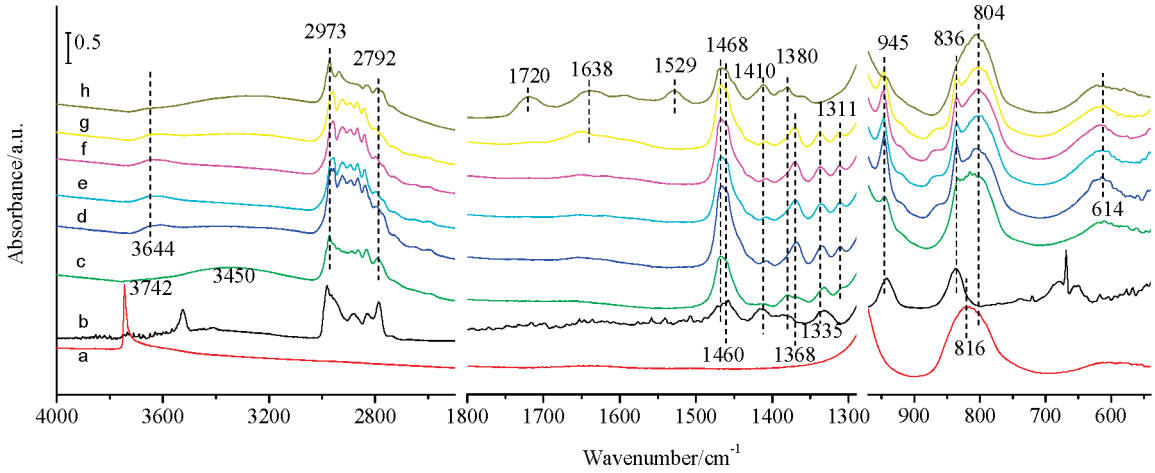

Figure 1. IR spectra of (a) MCM-41 dehydrated at 773 K, (b) pure copper precursor, and (c) Cu[OCHMeCH$_2$NMe$_2$]$_2$-adsorbed MCM-41 after removing the solvent at 298 K, (d) heating followed by eliminating the unreacted precursor at 353, (e) 373, (f) 393, (g) 423, and (h) 443 K.

obtain the structural parameters including interatomic distances (R), coordination numbers (CN), Debye−Waller factors ($\Delta\sigma^2$), and edge energy shifts (ΔE_0). The validity of each fit was checked by fitting of K^3-weighted spectra in k space. The quality of each fit was estimated from the values of the variances of the imaginary and absolute parts of the FT.

6. Thermal Behavior. Thermogravimetric-differential thermogravimetric (TG-DTG) analysis was performed using a PE TGA7 under a nitrogen flow rate of 20 cm^3·min^{-1} with a heating rate of 5 K·min^{-1}.

7. XPS Measurement. X-ray photoelectron spectra (XPS) were measured with a Quantum 2000 spectrometer with monochromatized Al Kα X-rays ($h\nu$ = 1486.6 eV) operating at 150 W. A sheet sample sealed in a glass tube was transferred and mounted on a stainless-steel sample holder with double-sided adhesive carbon tape in a glovebox with an Ar atmosphere. The original peak of the precursor was fitted into three components according to its structure and then calibrated by the BE (284.8 eV) of the C−C component to correct the binding energies of the other elements. As for the other samples, the electron BE (103.7 eV) of Si 2p in pure calcined MCM-41, calibrated by the BE of the C-(C, H) component (BE = 284.8 eV) coming from contamination carbon, was used as an internal standard.[31]

8. Temperature-Programmed Decomposition (TPD) Experiment. TPD was performed with an Autochem 2920 automatic catalyst characterization system equipped with an Omnistar GSD 30103 mass spectrometer. The sample loading was 0.2000 g. The flow rate of the carrying gas (highly pure He (5N)) was 30 cm^3·min^{-1}, and the heating rate was 5 K·min^{-1}.

Results

1. Chemical Adsorption of Cu[OCHMeCH$_2$NMe$_2$]$_2$ on the Surface of MCM-41: In Situ IR Study. After being treated under dynamic vacuum at 773 K for 4 h, MCM-41 shows only a strong vibration absorption band at 3742 cm^{-1} assigned to isolated silanol groups (Figure 1a).[32,33] Introducing a small amount of Cu[OCHMeCH$_2$NMe$_2$]$_2$ solution into the reactor, followed by eliminating the solvent by evacuation at room temperature, results in complete disappearance of the silanol band (Figure 1c) and appearance of a new weak and broad absorption at ca. 3450 cm^{-1}, thus indicating hydrogen bonding between the OH groups and the copper precursor. New C−H absorption bands in the 3000−2700 cm^{-1} region and at 1460, 1381, 1335, 945 and 836 cm^{-1}, which are in good agreement with those of the used copper precursor (Figure 1b),[23,34,35] are also clearly observed. It further indicates that the copper precursor is physically adsorbed on the surface of MCM-41.

Remarkable changes are observed after heating the above system at 353 K for 10 h and eliminating the physisorbed precursor under dynamic vacuum at such a temperature (Figure 1d). First, all of the C−H absorption bands in the 3000−2700 and 1500−1300 cm^{-1} regions increase considerably in intensity, and the hydrogen-bonded hydroxyl band narrows and shifts from 3450 to 3644 cm^{-1}. Simultaneously, the band at 816 cm^{-1} in the IR fingerprint range, belonging to the Si−O−Si distortion bending vibration mode,[36] shifts to 804 cm^{-1} due to this chemical interaction, and the Cu−O symmetric stretching mode at 614 cm^{-1} [37] becomes more intense, which is probably indicative of formation of Si−O→Cu bonds. These results show unambiguously that a strong chemical interaction of the Cu[OCHMeCH$_2$NMe$_2$]$_2$ molecules with the surface hydroxyls of MCM-41 occurs at this temperature.

A further experiment was performed with a higher amount of MCM-41 in order to determine quantitatively the evolved products and the chemical composition of the solid. Interestingly, no gaseous products were detected with both GC-MS and IR spectroscopy during heating at 353 K. Chemical

(31) Romanenko, A. V.; Kuznetsov, V. L.; Shepelin, A. P.; Zaikovskii, V. I.; Zhdan, P. A.; Plyasova, L. M.; Yermakov, Y. I. *React. Kinet. Catal. L* **1982**, *21*, 55–58.
(32) Chen, J.; Li, Q.; Xu, R.; Xiao, F. *Angew. Chem., Int. Ed. Engl.* **1995**, *34*, 2694–2696.
(33) Fripiat, J. J.; Uytterhoeven, J. *J. Phys. Chem.* **1962**, *66*, 800–805.
(34) Barraclough, C. G.; Bradley, D. C.; Lewis, J.; Thomas, I. M. *J. Chem. Soc.* **1961**, 2601.
(35) Singh, J. V.; Baranwal, B. P.; Mehrotra, R. C. *Z. Anorg. Allg. Chem.* **1981**, *477*, 235–240.
(36) Chen, L. F.; Noreňa, L. E.; Navarrete, J.; Wang, J. A. *Mater. Chem. Phys.* **2006**, *97*, 236–242.
(37) Adıgüzel, H. İ; İzgi, T. *J. Supercond.* **2002**, *15*, 549–551, Cu−O vibrations appear at 614 cm^{-1}; however, it broadens after being adsorbed on the surface of the support, indicating formation of Si−O→Cu bands.

Scheme 1. Reaction Process for $Cu[OCHMeCH_2NMe_2]_2$ Interacting with MCM-41

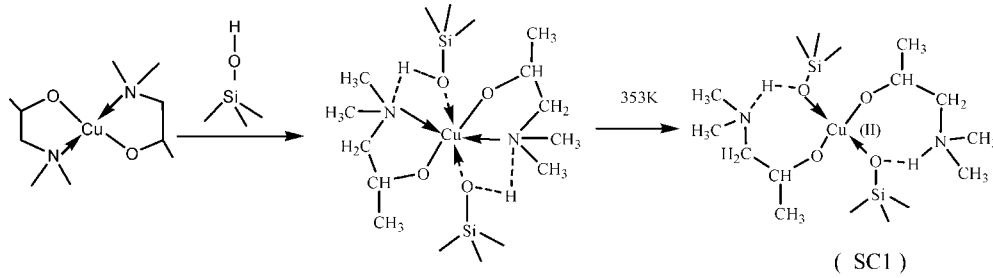

analysis of the resulting solid after complete elimination of the physisorbed species gives a C/Cu ratio of 10.7 and a N/Cu ratio of 2.38 (C, 3.18 wt %; N, 0.82 wt %; Cu, 1.56 wt %), close to those of the copper precursor $Cu[OCHMeCH_2NMe_2]_2$. This indicates no loss of organic ligands. It is therefore concluded that the $Cu[OCHMeCH_2NMe_2]_2$ molecule is fully bound onto the MCM-41 surface via the chemical interaction with the surface hydroxyl groups to form a surface-bound complex (denoted as SC1) as illustrated in Scheme 1. Such a surface-bound complex is relatively stable below 423 K, as shown by the lack of change in the IR spectra (Figure 1e and 1f). However, a new absorption, which will be assigned below, appears at 1650 cm^{-1} upon heating at 423 K (Figure 1g), indicating that thermolysis of SC1 starts at this temperature.

XAFS Analytical Results Regarding the Local Structure of the Surface Copper Complex 1. The local structure of the surface copper complex 1 is further characterized by X-ray absorption spectroscopy. Cu K-edge XAFS data were obtained for the copper precursor and the surface copper complex 1. The normalized XANES spectra collected at the Cu K-edge for these two samples are shown in Figure 2. For the copper precursor, an intense pre-edge absorption at 8.978 KeV corresponding to the electric quadrupole-allowed 1s → 3d transition is experimentally observed.[38] The 1s → 3d transition is sensitive to the coordination environment around the absorber and gains additional intensity in a noncentrosymmetric environment through mixing of Cu 3d and 4p as the transition of the 1s electron to the 4p electron is electric dipole allowed and therefore very intense.[39,40] The precursor $Cu[OCHMeCH_2NMe_2]_2$ is a typical square-planar

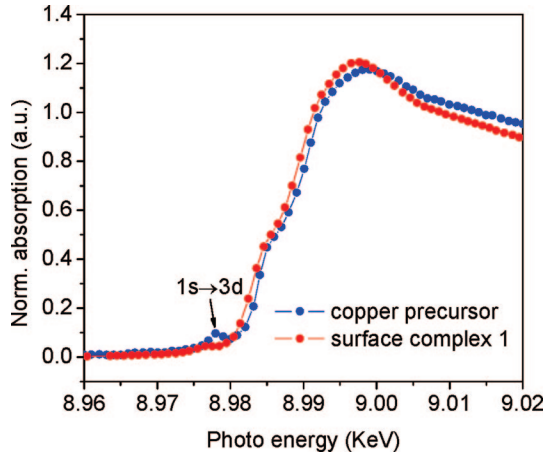

Figure 2. Normalized Cu K-edge XANES spectra of the surface copper complex and the copper precursor.

complex, the center copper atom of which is coordinated to two nitrogen atoms with a Cu−N distance of 2.03 Å and two oxygen atoms with a Cu−O distance of 1.86 Å.[22] One can conclude that the intense 1s → 3d peak of the precursor mainly originates from the noncentrosymmetric geometry of the Cu atom. Interestingly, the pre-edge feature becomes very weak for the surface copper complex 1 prepared by adsorption of $Cu[OCHMeCH_2NMe_2]_2$ on MCM-41 along with posttreatment in vacuum at 353 K, suggesting that a change of symmetry from the noncentrosymmetric geometry in $Cu[OCHMeCH_2NMe_2]_2$ to a centrosymmetric environment is the most likely cause of the decrease in intensity of the pre-edge feature, that is, the Cu−N coordination bonds may be ruptured and the N ligands are replaced by O atoms of hydroxyl groups of the support MCM-41 to form a relatively centrosymmetric surface complex as shown in Scheme 1. However, to further verify this observation, detailed analysis of the EXAFS data need to be undertaken.

The Cu K-edge K^3-weighted EXAFS spectra from the surface copper complex **1** together with the copper precursor are shown in Figure 3. All FT's are uncorrected for phase shifts. The FT of the copper precursor serves as a standard to estimate relative changes between samples. It can be seen from Figure 3 that the first peak in the FT of the data is shifted to a lower radical distance for the surface copper complex 1 relative to the copper precursor. This shift indicates a change in the first-shell peak distance. The first peak at about 1.5 Å (uncorrected), which is presumably due to two Cu−N and Cu−O shells from $Cu[OCHMeCH_2NMe_2]_2$, was back-filtered through a range of 1.0−2.1 Å, although this gives a poor fit. However, if the Cu−N shell is substituted with a Cu−O shell, a good fit can be achieved with a Cu−O distance of 1.89 Å and a Cu−O distance of 1.97 Å. Analysis of the Cu K-edge EXAFS data of the surface complex 1 gives a first coordination sphere of two O atoms at 1.89 Å and two O atoms at 1.97 Å. Although the quality of the data certainly limits the precision of this distant shell, these two Cu−O distances in the SC1 are distinctly longer than that (1.86 Å) of the precursor reported in the literature[22] and that (1.83 Å) of the precursor obtained by XAFS (see Table S1 in the Supporting Information). This further verifies formation of the surface complex shown in Scheme 1 (Table 1).

(38) Drake, I. J.; Fujdala, K. L.; Bell, A. T.; Tilley, T. D. *J. Phys. Chem. B* **2004**, *108*, 18421–18434.
(39) DuBois, J. L.; Mukherjee, P.; Hedmn, Britt.; Hodgson, K. O. *J. Am. Chem. Soc.* **2000**, *122*, 5775–5787.
(40) Kau, L. S.; Spira-Solomon, D. J.; Penner-Hahn, J. E.; Hodgson, K. O.; Solomon, E. I. *J. Am. Chem. Soc.* **1987**, *109*, 6433–6442.

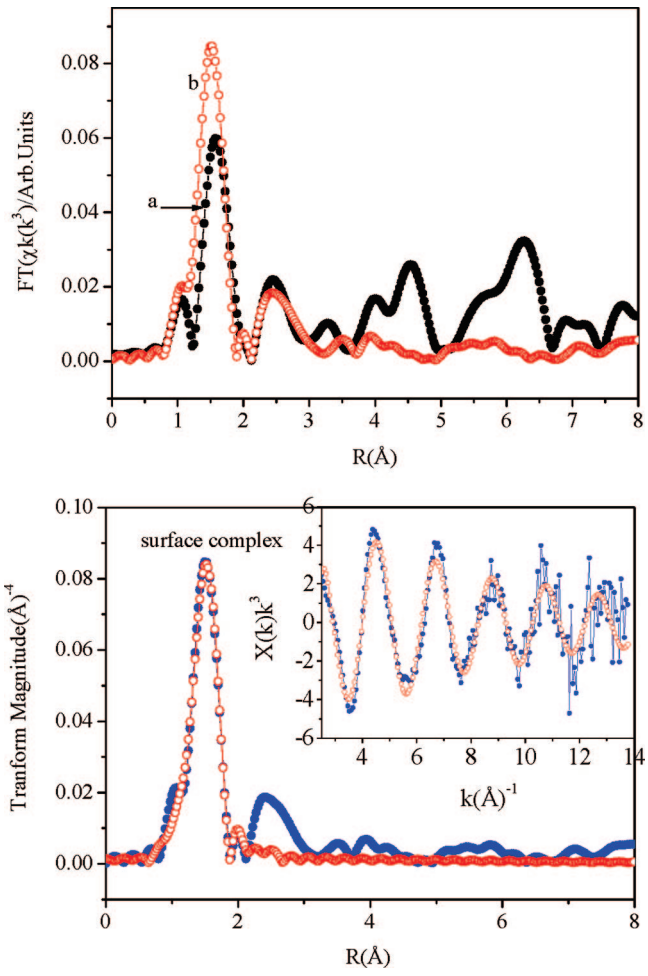

Figure 3. Cu K-edge EXAFS spectra of copper precursor (a) and the surface copper complex (b) reacted at 353 K.

Table 1. EXAFS Fit Parameters Characterizing the Surface Copper Complex 1[a]

sample	shell	CN	R, Å	σ^2, Å^2	ΔE_0, eV
CuO	Cu−O$_1$	2.0	1.93	0.003	3.4
	Cu−O$_2$	2.0	1.99	0.006	15.2
surface copper complex 1	Cu−O$_1$	2.0	1.89	0.003	7.7
	Cu−O$_2$	2.0	1.97	0.019	7.0

[a] Notes: CN, coordination number; R, absorber−backscatter distance; σ^2, Debye−Waller factor relative to that of the reference compound; and ΔE_0, inner potential correction. The approximate experimental uncertainties: CN, ±10%; R, ±10%.

2. Thermolysis of the Surface-Bound Cu Complex: In Situ IR Study. When SC1 is heated with evacuation in the temperature range 393−723 K, the IR spectra in the region 4000−2500 cm^{-1} change drastically (Figure 4). The C−H absorption bands in the region 3000−2700 cm^{-1} decrease remarkably in intensity, accompanied by the stepwise recovery of the isolated hydroxyl band at 3742 cm^{-1}, which indicates that loss of organic ligands occurs in this temperature range. By measuring the total integrated intensity of the bands in the region 3000−2700 cm^{-1}, a stepwise decrease in the C−H stretching band intensity (representing the amount of organic ligands) with increasing temperature is obtained and shown in Figure 5. It is clearly observed that thermolysis of SC1 occurs in two steps in the temperature range from 393 to 723 K. The first decomposition occurs in the temperature range 393−443 K and loses the majority of organic species, as indicated by the considerable decrease in the C−H stretching band intensity, whereas in the temperature range 473−523 K less loss of organic ligand suggests formation of another relatively stable copper intermediate complex (denoted as SC2). Such a SC2 undergoes the second decomposition step until complete loss of organic ligand upon heating at temperatures beyond 523 K (Figure 4f, 4g, 4h, and 4i). The stepwise changes above can also be well identified in the temperature range from 393 to 723 K by the IR spectra in the region 2200−1300 cm^{-1}. When SC1 is heated at 443 K, the C−H absorption bands in the range 2200−1300 cm^{-1} decrease considerably in intensity (Figure 4c), followed by the appearance of some new bands at 1720, 1638, and 1529 cm^{-1}. A lack of change in intensity of these bands is observed except that the 1529 cm^{-1} band shifts to 1578 cm^{-1} in the temperature range 443−523 K (Figure 4d and 4e). These observations are clearly different from those of SC1 and the used Cu precursor, which further indicates that SC1 is decomposed to form SC2 bound to the MCM-41 surface in this temperature range. SC2 contains both the carbonyl group and the C═N double bond, as characterized by the band at 1720 cm^{-1} belonging to the C═O group and the C═N bands at 1638, 1529, and 1578 cm^{-1}.[41–43] When the reaction temperature is beyond 523 K, the C═O and C═N bands gradually disappear along with the appearance of some bands at 1560, 2215, and 2245 cm^{-1}. These bands are indicative of formation of a C≡N bond (Figure S3 in the Supporting Information).[44,45] It is therefore inferred that SC2 is probably transformed into a novel organic species containing a nitrile structure (−C≡N) coordinated to the central Cu atom.[46] Beyond 723 K, the organic ligands are completely lost and a majority of the silanol groups come back (Figure 4i).

The evolved organic species are also identified by IR spectroscopy during heating in the temperature range 393−723 K. As shown by the difference IR spectra in the region 1300−1800 cm^{-1} before and after evacuation at 323 K in Figure 6, clearly, the IR spectra of evolved organic species are basically in agreement with that of the used Cu precursor after heating at temperatures below 423 K (Figure 6a and 6b), which is mainly attributed to desorption of the Cu precursor, whereas organic species evolved at the temperature region of 443−523 K represent completely different IR spectra. The appearance of an intense band at 1720 cm^{-1} indicates that the evolved fragments contain a carbonyl band (Figure 6B(c−e)).[47] The inverse band at 1529 cm^{-1} indicates formation of a double bond. Upon heating at temperatures beyond 523 K, the evolved products are some small molecules as no obvious characteristic peaks are observed in the difference spectra. Simultaneously, surface Cu complex

(41) Bahçecı, Ş.; İnce, N.; İkızler, A. *Turk. J. Chem.* **1998**, *22*, 237–241.
(42) Navneet, A.; Pradeep, M. *J. Zhejiang. Univ. SCI* **2005**, *6B*, 617–621.
(43) Doz, P.; Schröder, D. G. *Angew. Chem., Int. Ed.* **1965**, *4*, 695–696.
(44) Khairullin, V. K.; Vasyanina, M. A.; Pudovik, A. N. *Russ. Chem. B* **1967**, *16*, 1541–1542.
(45) Biak, N.; Atay, T. *Turk. J. Chem.* **1998**, *22*, 261–266.
(46) Mutsukura, N. *Diamond Relat. Mater.* **2001**, *10*, 1152–1155.
(47) Zaki, M. I.; Hasan, M. A.; Pasupulety, L. *Langmuir* **2001**, *17*, 768–774.
(48) Márquez, F.; Palomares, A. E.; Rey, F.; Corma, A. *J. Mater. Chem.* **2001**, *11*, 1675–1680.

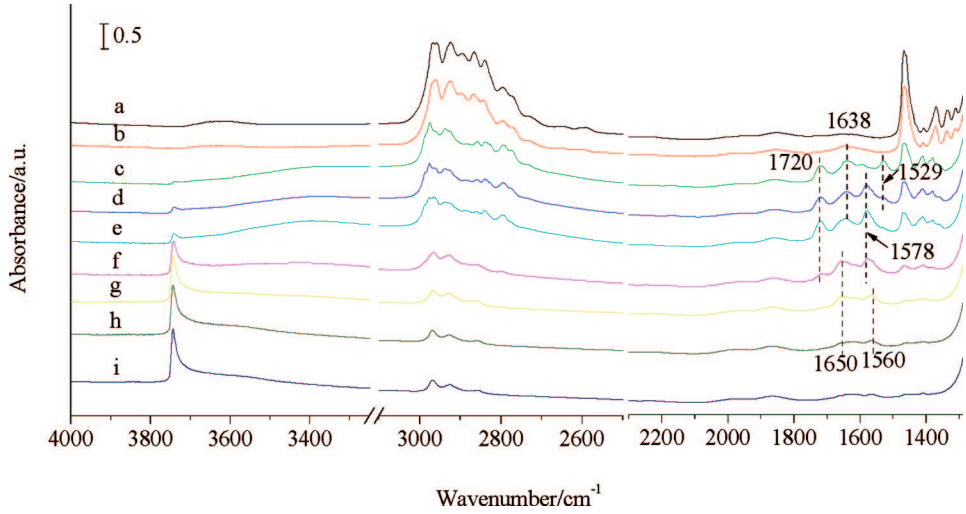

Figure 4. IR spectra of the $Cu[OCHMeCH_2NMe_2]_2$-adsorbed MCM-41 prepared at 353 K after heating at various temperatures and then evacuating at 323 K for 30 min: (a) 423, (b) 443, (c) 473, (d) 523, (e) 573, (f) 623, (g) 673, and (h) 723 K.

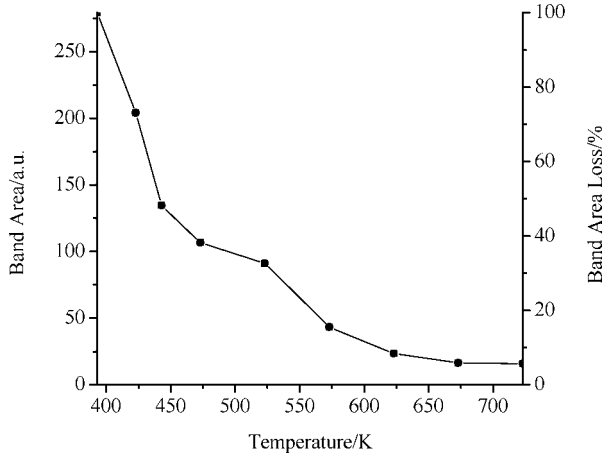

Figure 5. IR area in the region of 3000−2700 cm^{-1} with increasing temperature.

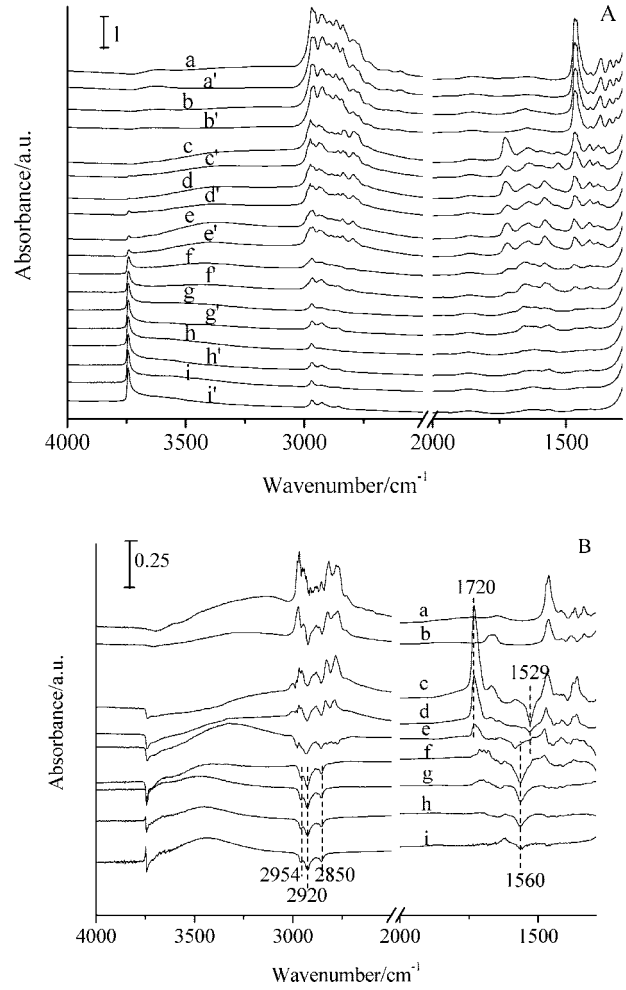

Figure 6. (A) Comparison of the IR spectra of the $Cu[OCHMeCH_2NMe_2]_2$-adsorbed MCM-41 at various temperatures (according to Figure 2) before (x) and after (x′) evacuation at 323 K. (B) Difference spectra (substracting the latter from the former) vs temperature: (a) 393, (b) 423, (c) 443, (d) 473, (e) 523, (f) 573, (g) 623, (h) 673, and (i) 723 K.

with methyl groups and nitrile groups have been formed (seeing some inverse IR absorptions band at 2954, 2850, and 1560 cm^{-1}). Complete loss of surface complex is at temperatures beyond 723 K.

TG-DTG Analysis. Figure 7 shows the TG plots for the Cu complex-bound MCM-41 sample prepared at 353 K and the parent copper precursor. For the parent precursor, it is evident that only one-step weight loss occurs between 383 and 463 K in the DTG curve (Figure 7A), which parallels the results reported in the literature,[24] whereas the Cu complex-bound MCM-41 exhibits a different DTG curve compared with that of the pure copper precursor (Figure 7B). Two separated weight losses can be clearly observed. The first weight loss occurs between 423 and 523 K and accounts for ca. 65% of the total weight loss, while the second one is between 523 and 723 K and possesses ca. 35% of the total weight loss. This is in quite good accordance with the results from the IR spectra above.

TPD-MS. Figure 8 represents the TPD-MS pattern of the Cu complex-adsorbed MCM-41. The most important fragments detected between 423 and 723 K are $CH_3C{=}OCH_2NMe_2$ (*m*/*z* 101), CH_2NMe_2 or CH_3COCH_3 (*m*/*z* 58), $CH_3C{=}OCH_2$ (*m*/*z* 57), NMe_2 (*m*/*z* 44), $CH_3C{=}O$ (*m*/*z* 43), $CH{=}NCH_3$ (*m*/*z* 42), $C{=}O$ (*m*/*z* 28), CH_3 (*m*/*z* 15), etc., with no evidence for $CH_3CH(OH)CH_2NMe_2$ (*m*/*z* 103), which indicates that decomposition of SC1 occurs in this temperature range. The TPD patterns of all organic fragments

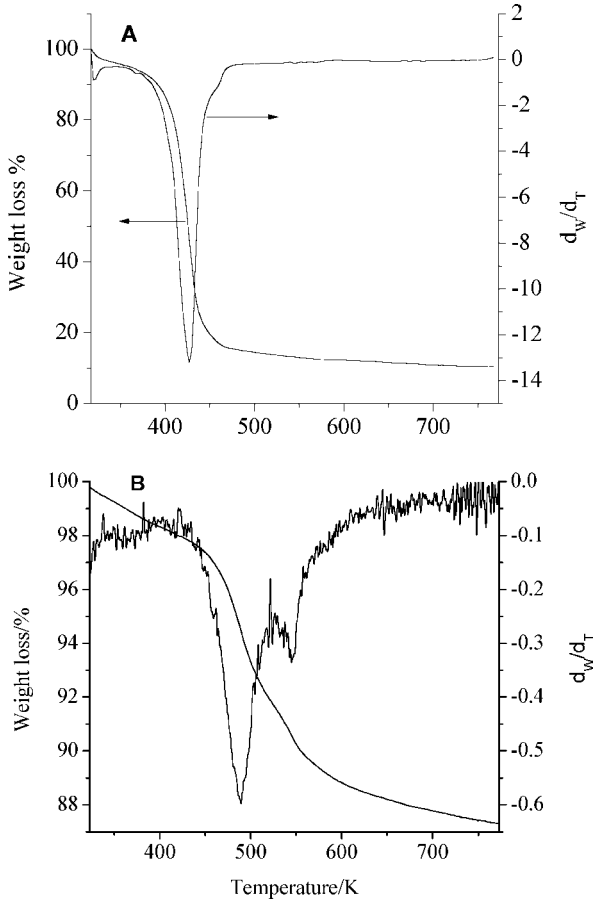

Figure 7. TG and DTG spectra of Cu[OCHMeCH$_2$NMe$_2$]$_2$ (A) and the Cu[OCHMeCH$_2$NMe$_2$]$_2$-adsorbed MCM-41 prepared at 353 K (B).

(except CH$_3$C═OCH$_2$NMe$_2$ *m/z* 101) present double release peaks. Interestingly, the area ratio of the peak centered at 468 K and that centered at 588 K is close to 1:1 for the total sum of all of fragments with a decomposition onset temperature of 423 K. This clearly indicates that SC1 remains intact below 423 K and undergoes two-step decomposition beyond 423 K, which is in good agreement with the results from IR and TG characterizations.

However, it can be clearly seen that the first-step decomposition below 523 K is different from the second-step decomposition. As shown in Figure 8, the major fragment is CH$_2$NMe$_2$ (*m/z* 58; Table 2) in the temperature range 423−523 K (first-step), while the CH═NCH$_3$ (*m/z* 42) fragment is predominant in the temperature range 523−723 K (second-step). Moreover, the maximal fragments detected in the temperature ranges of 423−523 and 523−723 K are CH$_3$C═OCH$_2$N(CH$_3$)$_2$ (*m/z* 101) and an organic complex with a *m/z* ratio of 85, respectively. This shows that the first-step decomposition causes one ligand to be oxidized to CH$_3$C═OCH$_2$N(CH$_3$)$_2$ and the divalent Cu atom to be reduced to Cu^+. Residual ligand coordinated to Cu^+ is not CH$_3$CH(OH)CH$_2$NMe$_2$ (*m/z* 103) but the organic complex with a *m/z* ratio of 85 (SC2). The ligand possesses ca. 35 wt % of the total organic ligands of the Cu precursor, which is in good agreement with the TG results mentioned above. Smaller molecular weight products such as CH$_2$NMe$_2$ (*m/z* 58), CH$_3$C═OCH$_2$ (*m/z* 57), N(CH$_3$)$_2$ (*m/z* 44), and other fragments can be derived from the thermal decomposition

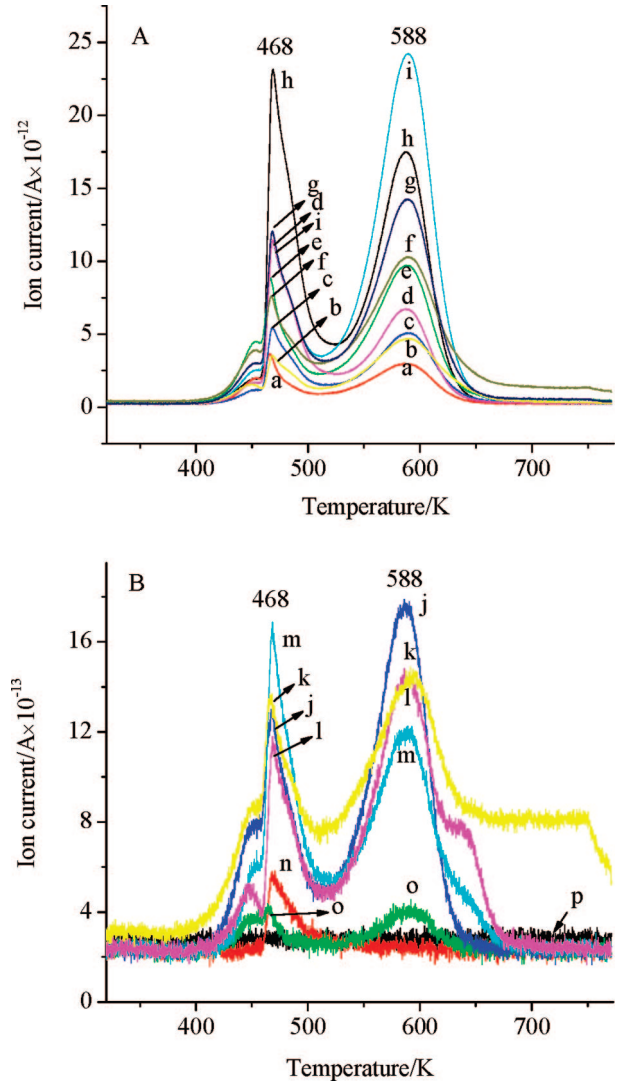

Figure 8. TPD-MS plots of the Cu[OCHMeCH$_2$NMe$_2$]$_2$-adsorbed MCM-41 prepared at 353 K: *m/z* = (a) 45, (b) 29, (c) 43, (d) 30, (e) 44, (f) 28, (g) 15, (h) 58, (i) 42, (j) 59, (k) 16, (l) 56, (m) 57, (n) 101, (o) 85, and (p) 103.

Table 2. Different *m/z* Values and the Corresponding Fragments

m/z	fragment	*m/z*	fragment
103	CH$_3$CH(OH)CH$_2$NMe$_2$	45	NH(CH$_3$)$_2$
101	CH$_3$C═OCH$_2$NMe$_2$	44	NMe$_2$
85	CH$_3$N═CHC═OCH$_3$	42	CH$_3$N═CH
56	CHC═OCH$_3$	43	CH$_3$C═O
59	CH$_3$C═OH$^+$CH$_3$	30	HCHO
58	CH$_3$C═OCH$_3$ or CH$_2$NMe$_2$	57	CH$_3$C═OCH$_2$ or CH$_3$N═CHCH$_3$
29	NCH$_3$	28	C≡O
16	CH$_4$	15	CH$_3$

of CH$_3$C═OCH$_2$N(CH$_3$)$_2$ (c.f. its mass spectrum from http://www.aist.go.jp).

To further confirm the SC2 species, the sample prepared via heating the Cu complex adsorbed MCM-41 at 473 K for 2 h and eliminating the physisorption species is used to TPD experiment. The result shows in Figure 9. It is clearly seen that single-release peaks occur between 523 and 723 K, which is fully consistent with the second desorption peaks of the Cu complex-adsorbed MCM-41 sample. The first-step decomposition in the temperature range of 423−523 K almost disappears after thermal treatment at a temperature of 473 K. This indicates that one ligand of the SC1 bonded

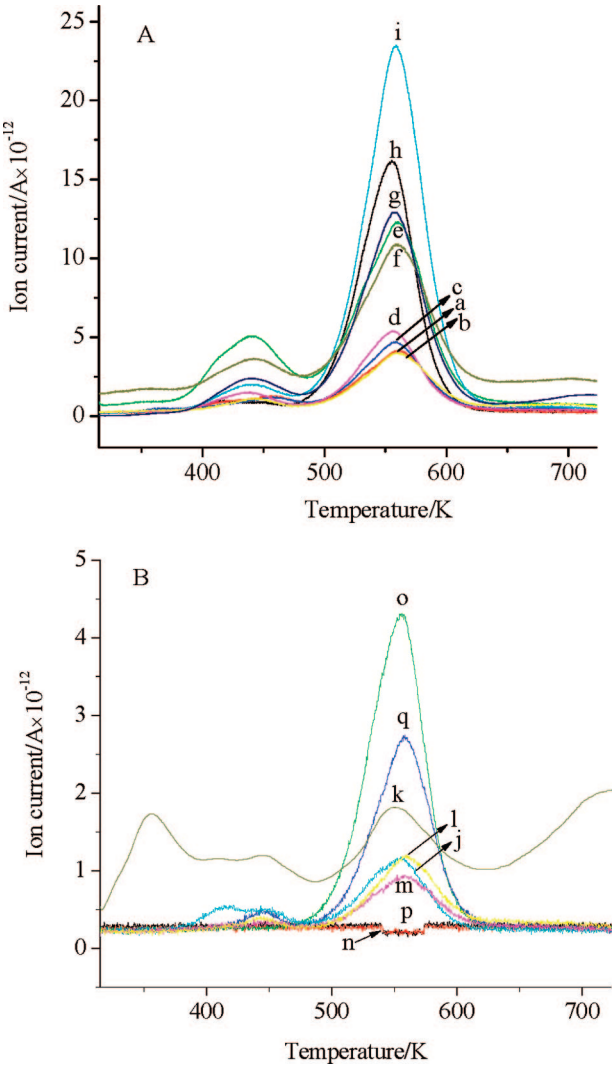

Figure 9. TPD-MS plots of the sample prepared via heating the Cu-complex-adsorbed MCM-41 at 473 K for 2 h and eliminating the physisorption species: m/z = (a) 45, (b) 29, (c) 43, (d) 30, (e) 44, (f) 28, (g) 15, (h) 58, (i) 42, (j) 59, (k) 16, (l) 56, (m) 57, (n) 101, (o) 85, (p) 103, (q) 70, and (r) 27.

on MCM-41 is eliminated via an autoredox reaction to form a relatively stable intermediate (SC2) after heating at 473 K. This further proves the IR and TG results above. The fragments detected between 523 and 723 K are $CH{=}NCH_3$ (m/z 42), CH_3COCH_3 (m/z 58), CH_3 (m/z 15), C═O (m/z 28), $CH_3COCH{=}NCH_3$ (m/z 85), $COCH{=}NCH_3$ or CH_3-$COCH{=}N$ (m/z 70), etc., with no evidence for CH_3-$COCH_2N(CH_3)_2$ (m/z 101) or $CH_3CH(OH)CH_2N(CH_3)_2$ (m/z 103). This in combination with the IR observations suggests that the $CH_3COCH{=}NCH_3$ fragment is possibly the ligand molecule coordinated to the Cu atom for the following reasons: first, $CH_3COCH{=}NCH_3$ contains both a carbonyl and a double bond, which can explain the above-described IR observations. Second, $CH_3COCH{=}NCH_3$ has a quasi-Schiff base structure and can coordinate with transition metals with a vacant orbital to form a stable organometallic complex. Finally, the $CH_3COCH{=}NCH_3$ ligand is easily decomposed to small molecule fragments, such as $CH{=}NCH_3$, CH_3, $COCH{=}NCH_3$ or $CH_3COCH{=}N$, and $CH{\equiv}N$, which shows that the third surface complex (SC3) contains the $-C{\equiv}N$ bond, which is consistent with the IR results.

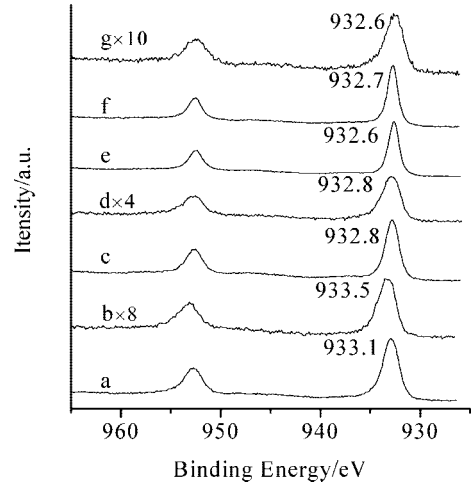

Figure 10. XPS spectra of Cu 2p of (a) the precursor and the copper species containing MCM-41 obtained at (b) 353, (c) 443, (d) 473, (e) 493, (f) 623, and (g) 773 K.

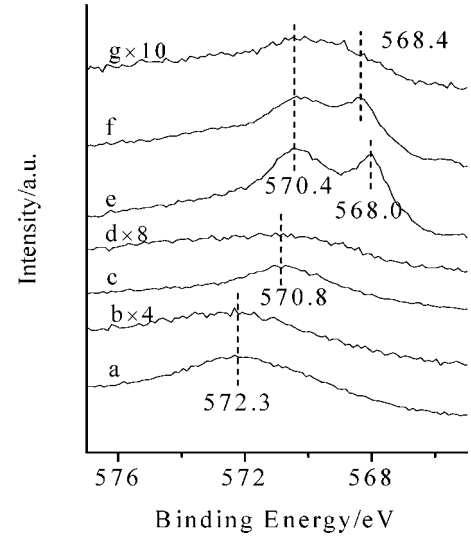

Figure 11. XPS spectra of Cu LMM of (a) the precursor and the copper species containing MCM-41 obtained at (b) 353, (c) 443, (d) 473, (e) 493, (f) 623, and (g) 773 K.

Unfortunately, we have not found MS spectra of $CH_3N{=}CHCOCH_3$ in the literature.

X-ray Photoelectron Spectroscopy Characteristics. Chemical state change of surface copper complexes formed with increasing temperature was monitored by X-ray photoelectron spectroscopy. XPS spectra of Cu2p, Cu LMM Auger spectra, and XPS spectra of N1s obtained are shown in Figures 10, 11, and 12, respectively. The binding energies of $Cu2p_{3/2}$ and $Cu2p_{1/2}$ are 952.7 and 933.1 eV, respectively, for the Cu precursor (Figure 10a), which are close to those of CuO,[49–51] thus indicating that the central copper atom is in the divalent state. When the Cu precursor is introduced into MCM-41 along with thermal treatment at 353 K, the binding energies of $Cu2p_{3/2}$ and $Cu2p_{1/2}$ increased to 953.1

(49) Gervasini, A.; Manzoli, M.; Martra, G.; Ponti, A.; Ravasio, N.; Sordelli, L.; Zaccheria, F. *J. Phys. Chem. B* **2006**, *110*, 7851–7861.
(50) Mclntyre, N. S.; Cook, M. G. *Anal. Chem.* **1975**, *47*, 2208–2213.
(51) Tobin, J. P.; Hirschwald, W.; Cunningham, J. *Appl. Surf. Sci.* **1983**, *16*, 441–452.
(52) Robert, T.; Bartel, M.; Offergeld, G. *Surf. Sci.* **1972**, *33*, 123–130.

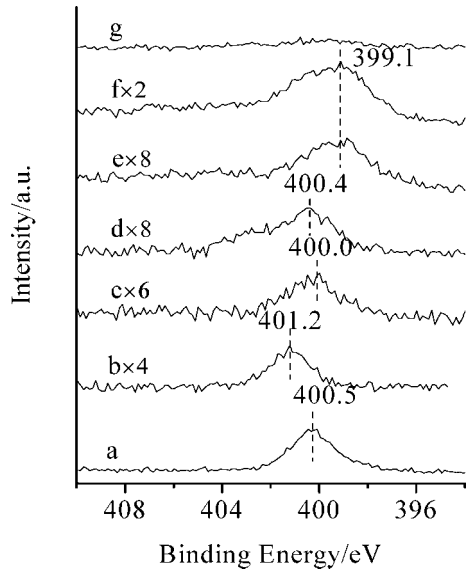

Figure 12. XPS spectra of N1s of (a) the precursor and the copper species containing MCM-41 obtained at (b) 353, (c) 443, (d) 473, (e) 493, (f) 623, and (g) 773 K.

and 933.5 eV, respectively (Figure 10b). This shift toward high energy is strongly indicative of the decrease in the electron density of Cu atom, thus further validating the aforementioned conclusion from IR observation and XAFS results that transformation of the coordination bond Cu←N into Cu←O occurs at such a temperature. Upon heating at 443 K, even at higher temperature, the BE of Cu2p$_{1/2}$ decrease from 933.5 to ca. 932.8 (Figure 10c−g), showing that the Cu^{2+} atom is reduced to Cu^{+} or metal Cu, [53] accompanied by oxidation and decomposition of ligands as shown by the IR results.

It can be more clearly observed from the Cu LMM Auger spectra that reduction of Cu^{2+} in the temperature range 353−773 K undergoes two steps (Figure 11). Thermal treatment below 353 K does not lead to a change in the chemical state of the Cu complex bound on MCM-41 as indicated by no change of the LMM peak at 572.3 eV (Figure 11a and 11b). This means that copper still is in the Cu^{2+} state, whereas the first-step reduction occurs between 353 and 443 K (Figure 11b and 11c). The shift of the LMM peak from 572.3 to 570.8 eV indicates formation of Cu(I).[54] At temperatures beyond 493 K (Figure 11e−g) the second-step reduction of Cu^{+} to Cu is distinctly observed as shown by the appearance of a metallic copper peak at ca. 568.0 eV.[54]

The N 1s XPS spectra shown in Figure 12 also give important information on the structural change of the ligand coordinated to the Cu atom with increasing temperature. The binding energy of the N1s peak of the N atom coordinated to metallic copper is 400.5 eV for the Cu precursor (Figure 12a), which is the same as that reported in the literature,[55] whereas it shifts to 401.2 eV when the precursor was adsorbed onto MCM-41 along with thermal treatment at 353 K (Figure 12b). It indicates formation of $[HNR_3]^{\delta+}$ species.[56] When the reaction temperature increases to 443 and 473 K, the N1s peak occurs at 400.0−400.5 eV (Figure 12c and 12d), which is close to that of the N atom of the N−sp^{2}C bond,[57,58] indicating the occurrence of a C═N double bond at such a temperature. Heating at 493 and 623 K results in a further decrease in the binding energy of N1s to 399.1 eV (Figure 12e and 12f), which is consistent with that of the N atom of C≡N (nitrile).[59] No functional group containing nitrogen is left on the surface of the support at 773 K. These results are in good agreement with the IR characterization.

Discussion

1. Chemically Adsorbed State of Cu[OCHMeCH$_2$NMe$_2$]$_2$ on MCM-41. Cu[OCHMeCH$_2$NMe$_2$]$_2$ is an extremely water-sensitive solid. Two ligands are bonded to the central copper via nitrogen (lone-pair coordination with the central metal ion) and oxygen (covalent bond with the central metal ion) with a Cu−O distance of 1.865 Å and a Cu←N distance of 2.025 Å, forming a distorted five-membered chelate complex.[22,23] MCM-41 is rich with isolated hydroxyls on its surface of the mesopore upon dehydration at 773 K. When the Cu precursor is introduced to the dehydrated MCM-41 and then heated at 353 K, the precursor is chemically adsorbed on the MCM-41 via the interaction between the surface hydroxyl and the central Cu atom of the Cu precursor, resulting in transformation of the Cu←N bond into a Cu←O−H−N(Me$_2$)− bond to form a seven-membered ring chelate Cu complex containing an intramolecular hydrogen bond, as shown by the weak and broad absorption band at 3640 cm^{-1} in the IR spectra, which is indicative of the existence of the hydrogen bond in SC1, as shown in Scheme 1. This strong interaction is also confirmed by the reaction of Cu[OCHMeCH$_2$NMe$_2$]$_2$ with deuterated MCM-41(see Figure S1 in the Supporting Information).

Formation of such a surface complex 1 (SC1) is strongly supported by the experimental results as follows. (i) EXAFS results show that each copper atom is coordinated, on average, to two oxygen atoms with a Cu−O distance of 1.89 Å and to two oxygen atoms with a Cu−O distance of 1.97 Å. (ii) Introduction of the precursor Cu[OCHMeCH$_2$NMe$_2$]$_2$ followed by heating at the temperature results in complete disappearance of the isolated silanol of MCM-41 accompanied by the increase in intensity of the Cu−O band at 614 cm^{-1}. No gases are detected. (iii) Compared to those of the pure Cu precursor, the BEs of Cu2p shift by ca. 0.4 eV toward high energy and the BE of N1s shifts by ca. 0.7 eV toward high energy, while the Cu LMM spectra show that copper still exists in the divalent state. Some analogous surface complexes Cu(acac)$_2$ and Cu(hfac)$_2$ formed by the

(53) Moulder, J. F.; Stickle, W. F.; Sobol, P. E.; Bomben, K. D. *Handbook of X-Ray Photoelectron Spectroscopy*; Physical Electronics, Inc.: Chanhassen, MN,1995.
(54) Prissanaroon, W.; Brack, N.; Pigram, P. J.; Liesegang, J. *Surf. Interface Anal.* **2003**, *35*, 974–983.
(55) Auroux, A.; Gervasini, A.; Guimon, C. *J. Phys. Chem. B* **1999**, *103*, 7195–7205.
(56) Chan, H. S. O.; Neuendorf, A. J.; Ng, S. C.; Wong, P. M. L.; Young, D. J. *Chem. Commun.* **1998**, 1327–1328.
(57) Hiraoka, H.; Lee, W. Y. *Macromolecules* **1978**, *11*, 622–624.
(58) Crunteanu, A.; Charbonnier, M.; Romand, M.; Vasiliu, F.; Pantelica, D.; Negoita, F.; Alexandrescu, R. *Surf. Coat. Technol.* **2000**, *125*, 301–307.
(59) Toth, A.; Bell, T.; Bertoti, I.; Mohai, M.; Zelei, B. *Nucl. Instrum. Methods B* **1995**, *148*, 1131.
(60) Kenvin, J. C.; White, M. G.; Mitchel, M. B. *Langmuir* **1991**, *7*, 1198–1205.

Scheme 2. Decomposition Pathways for Surface Copper Complex

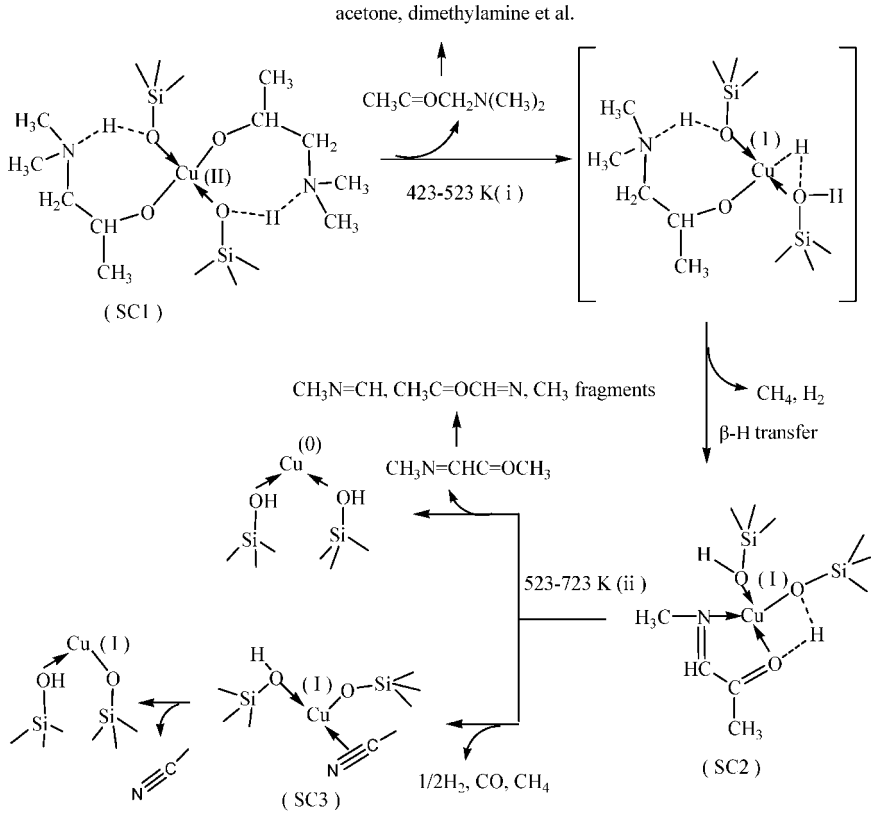

hydrogen-bonding interaction between the complex and isolated hydroxyls have been reported in the literature.[61,62] This surface complex 1 is relatively stable in natural air or in vacuum below 423 K, which is quite different from the parent copper precursor, as shown by IR spectra (Figure 1d−f).

2. Possible Thermolytic Pathway of Surface-Adsorbed Copper Species. All the results from IR, TG, TPD, and XPS show that surface complex 1 is decomposed in two steps at temperatures beyond 423 K. The stepwise pathway for the thermolysis of $Cu[OCHMeCH_2NMe_2]_2$ on the surface of MCM-41 can be well understood to occur as follows (Scheme 2). The surface complex 1 undergoes the first-step decomposition in the temperature range of 423−523 K, eliminating 1-dimethylamino-2-propanone via a β-hydrogen transfer toward the central Cu atom to transform into a novel surface copper complex 2 (SC2). Simultaneously, Cu^{2+} is reduced to Cu^{+}. In combination with the IR observation that the residual surface species has a ligand with C═N and C═O double bonds, we suggest that the SC2 may be a Cu complex with a ligand $CH_3N{=}CHCOCH_3$, which is formed via H_2 elimination followed by another β-hydrogen transfer and CH_4 elimination. $CH_3N{=}CHCOCH_3$, which has been detected by MS (*m*/*z* 85), is a Schiff base that easily coordinates with Cu by its −N═C group to form a relatively stable intermediate on the surface of MCM-41.[62] The formed SC2 suffers from the second decomposition in the temperature range 523−723 K, releasing some small molecules such as carbon monoxide and methane to form a surface copper species (SC3) with a C≡N (nitrile) bond, elimination of which at 723 K leads to Cu(I) oxide anchored to the surface by Cu−O−Si covalent bond, or losing the whole ligand $CH_3N{=}CHCOCH_3$ along with reduction of Cu^{+} species formed in the first step into metallic Cu species.

The proposed mechanism is distinctly different from the self-decomposition and MOCVD pathways already reported in the literature, despite the initial step being in agreement with that suggested by Young et al.[23] Thermolysis of $Cu(OCH_2CH_2NMe_2)_2$ and $Cu(OCHMeCH_2NMe_2)_2$ complexes reported first by Goel et al. formed copper metal phase as the only product for the later, while a mixture of copper (Cu, CuO, and Cu_2O) formed for the former at ambient pressure under a N_2 stream (298−573 K, 2 h).[22] Thermolysis of some Cu precursors without β-hydrogen, for example, $Cu(OC(CF_3)R^1CH_2NHR_2)_2$ ($R^1 = CF_3$ or Me, $R^2 = Bu$), was suggested to proceed via cleavage of the C(α)−C(β) bond to Cu(s), $CF_3(R^1)C{=}O$, $HC{=}NR_2$, and $HOC(CF_3)R^1$-CH_2NHR_2.[28] Moreover, Park et al. proposed that $Cu(OMe_2CH_2NR_2)_2$ (R = Me or Et) was thermally decomposed by the dialkylamino group assisted γ-hydrogen elimination reaction and a cooperative C(α)−C(β) bond fission reaction, followed by reductive elimination to result in Cu metal deposit accompanying formation of $Me_2NH{=}CHNMe_2$ and $Me_2NCH_2CMe_2OH$, whereas study of the MOCVD chemistry of these Cu complexes [$Cu(OCR_2$-$CH_2NMe_2)_2$ (R = H, CH_3) on supports including $SrTiO_3$, SiO_2/Si, and ZnO/MCM-41 showed that the β-hydride elimination and reductive elimination reactions are key steps leading to reduction of divalent Cu to metallic Cu.[23,24] These studies found that the thermally decomposed products and

(61) Farkas, J.; Smith, M. J. H.; Kodas, T. T. *J. Phys. Chem.* **1994**, *98*, 6753–6762.
(62) Singh, U. G.; Williams, R. T.; Hallam, K. R.; Allen, G. C. *J. Solid State Chem.* **2005**, *178*, 3405–3413.

courses of these Cu complexes are dependent on the ligand. However, all the suggested mechanisms were based on the analytical results from the cumulative reactor gas-phase products in the CVD process by IR or/and mass or/and NMR spectroscopy. Clearly, a quite incomplete and to some extent misleading picture of the thermolysis chemistry of organometallic copper complexes on supports can be obtained if only the gas-phase products are examined. As mentioned by Young et al., the reaction pathway cannot be established beyond doubt in their experimental system.[23] Our strategy used in this work is based on approach of surface organometallic chemistry,[63–65] which allows us to identify the reactive intermediates anchored on the support surface step by step and their change with increasing temperature during thermolysis of the Cu precursor. It can be more reasonably concluded that β-hydride elimination and subsequent reductive elimination are two key steps to control formation of Cu species for Cu(OCHMeCH$_2$NMe$_2$)$_2$.

3. Effect of Support MCM-41 on the Thermolysis of Cu[OCH(Me)CH$_2$NMe$_2$]$_2$. It can be certain that the difference between our suggested pathway and that reported in the literature is related to the presence of the support MCM-41. Compared to strontium titanate[23] and SiO$_2$/Si,[24] MCM-41 possessed a large amount of isolated surface hydroxyls following pretreatment.[66] The interaction between the hydroxyls and the copper precursor would modify the chemical performance of the Cu complex compared to its bare state, as shown by our results. (i) The Cu complex bonded to MCM-41 is decomposed via two independent and consecutive steps in which the SC2 and SC3 as corresponding intermediates are recognized, while for general the CVD process decomposition of the Cu precursor was suggested to be consecutive, although it undergoes both β-hydride elimination and reductive elimination. (ii) Thermolysis of the copper complex bonded to the MCM-41 surface leads to a mixture of Cu(0) and Cu(I), while thermolysis of the Cu precursor under an inert atmosphere generally obtained copper metal as the only phase. As shown in Scheme 2, the effects of MCM-41 on the decomposition can be explained by interaction between the surface hydroxyls and the Cu precursor. Cleary, our study emphasizes a pivotal role of surface hydroxyls of the support MCM-41 in controllable formation of Cu species.

(63) Lefebvre, F.; Mallmann, A.; Basset, J. M. *Eur. J. Inorg. Chem.* **1999**, 361–371.
(64) Copéret, C.; Chabanas, M.; Arroman, R. P. S.; Basset, J. M. *Angew. Chem., Int. Ed.* **2003**, *42*, 156–181.
(65) Long, J.; Wang, X.; Zhang, G.; Dong, J.; Yan, T.; Li, Z.; Fu, X. *Chem. Eur. J.* **2007**, *13*, 7890–7899.
(66) Jentys, A.; Kleestorfer, K.; Vinek, H. *Microporous Mesoporous Mater.* **1999**, *27*, 321–328.

Conclusion

The copper precursor Cu[OCHMeCH$_2$NMe$_2$]$_2$ is strongly adsorbed on the surface of MCM-41 by reaction with the hydroxyl groups to form a surface copper complex 1 with a seven-membered ring chelate structure. This surface copper complex is stable in vacuum below 423 K. However, it is easily decomposed into a mixture of Cu(I) and Cu(0) via a successive two-step pathway upon heating at temperatures beyond 423 K. In the first-step decomposition it is first transformed into surface complex 2 containing both C═O and C═N double bonds where copper exists in the Cu(I) state in the temperature range from 423 to 523 K and then surface complex 2 undergoes the second decomposition in the temperature range of 523−723 K, causing formation of a mixture of Cu(0) and Cu(I) where surface complex 3 containing a C≡N bond is responsible for Cu(I) formation. The surface hydroxyl groups participate in the adsorption and reaction of the Cu precursor on the support MCM-41, which is a critical factor for controllable preparation of Cu-containing MCM-41 catalysts.

Acknowledgment. This work was financially supported by the National Science Foundation of China (nos. 20673020, 20537010) and National Basic Research Program of China (973 Program 2007CB613306). The authors thank Prof. Shiqiang Wei and Drs. Bo He and Zhiyun Pan, Hefei Synchrotron Radiation Laboratory (NSRL) (University of Science and Technology of China, Hefei) for collection, discussion, and analysis of XAFS data.

Supporting Information Available: Additional information (PDF). This material is available free of charge via the Internet at http://pubs.acs.org.

CM7027228